Made in United States of America
Reprinted from METEORITICS
Vol. 29, No. 2, March 1994

The Mbale meteorite shower

PETER JENNISKENS[1,2,†], HANS BETLEM[1], JAN BETLEM[1], ERASMUS BARIFAIJO[3], THOMAS SCHLÜTER[3], CRAIG HAMPTON[3], MATTHIAS LAUBENSTEIN[4], JOACHIM KUNZ[4], AND GERD HEUSSER[4]

[1]Dutch Meteor Society, Lederkarper 4, NL-2318 NB Leiden, The Netherlands
[2]Leiden Observatory, P. O. Box 9513, NL-2300 RA Leiden, The Netherlands
[3]Department of Geology, Makerere University, P. O. Box 7062, Kampala, Uganda
[4]Max-Planck-Institut für Kernphysik, Postfach 103980, D-69029 Heidelberg, Germany
†Present address and to whom correspondence should be addressed: NASA/Ames Research Center, M.S. 239-4, Moffett Field, California 94035-1000, USA

(Received 1993 July 26; accepted in revised form 1993 December 21)

Abstract–On 1992 August 14 at 12:40 UTC, an ordinary chondrite of type L5/6 entered the atmosphere over Mbale, Uganda, broke up, and caused a strewn field of size 3 x 7 km. Shortly after the fall, an expedition gathered eye witness accounts and located the position of 48 impacts of masses between 0.1 g and 27.4 kg. Short-lived radionuclide data were measured for two specimens, one of which was only 12 days after the fall. Subsequent recoveries of fragements has resulted in a total of 863 mass estimates by 1993 October. The surfaces of all fragments contain fusion crust. The meteorite shower caused some minor inconveniences. Most remarkably, a young boy was hit on the head by a small specimen.

The data are interpreted as to indicate that the meteorite had an initial mass between 400–1000 kg (most likely ~1000 kg) and approached Mbale from Az = 185 ±15, H = 55 ± 15, and V_∞ = 13.5 ± 1.5/s. Orbital elements are given. Fragmentation of the initial mass started probably above 25 km altitude, but the final catastrophic breakup occurred at an altitude of 10–14 km. An estimated 190 ± 40 kg reached the Earth's surface minutes after the final breakup of which 150 kg of material has been recovered.

INTRODUCTION

The breakup of a meteorite in the lower atmosphere often results in a strewn field. The larger masses retain part of their cosmic velocity longer than the smaller ones and, therefore, are found further out along the ground-projected trajectory (*e.g.*, Krinov, 1960; Nininger, 1963; Heide, 1988). After correction for atmospheric winds, the pattern of the strewn field contains valuable information about the (pre-) atmospheric trajectory and the breakup process.

An accurate atmospheric trajectory and entry velocity have been determined by multistation photography of the meteor, but this method has been successful in only three meteorite falls (Ceplecha, 1961; McCrosky *et al.*, 1971; Halliday *et al.*, 1978). Less accurate data of another 12 falls exist from visual accounts. From a statistical analysis of these still scarce data, it has been concluded that the inclinations of the pre-atmospheric orbits tend to be higher on average than those of main-belt asteroids but are similar to those of near-Earth asteroids (Jenniskens *et al.*, 1992a).

The breakup process has been studied in detail for the large Jilin H5 chondrite, with a strewn field of 480 km², by using short-living radionuclides as tracers of the depth of a fragment in the initial body. It was concluded that the stone broke up gradually from the outside to the inside (Heusser *et al.*, 1985; Begemann *et al.*, 1985; Müller and Jessberger, 1985).

This paper presents the results of a field expedition which was held between 1992 August 29 and September 5 in order to study the strewn field of the Mbale meteorite which fell on August 14 of that year. During the expedition, eye witnesses of the meteor phenomena were interviewed, and 48 impact positions were located. Masses between 0.1 g and 27 kg were recovered, amounting to what is thought to be a significant part of the total fallen mass. Initial accounts are given in Betlem (1992, 1993) and Barifaijo *et al.* (1993). In this paper, we describe the circumstances of the fall, the distribution of masses in the strewn field, the size distribution of fragments, and determine the pre-entry orbit. With a strewn field of 3 x 7 km, the Mbale fall is a typical case for the initial mass range of 100–1000 kg (Heide, 1988).

THE DATA

This is the third recorded fall in Uganda. Earlier falls are the stony Maziba, of 4.975 kg, which fell near Kabale on 1942 September 24, and the iron Soroti meteorite, which fell in the Teso District on 1945 September 17 (Roberts, 1947). In the latter case, four pieces of a meteorite shower were recovered.

Visual Observations

The new fall occurred in a heavily populated area in and around the city of Mbale (λ = 34°09'35"E, ϕ = 1°04'01"N–main mass). A loud explosion was heard which persisted for some time as a rumbling noise at about 3:40 pm (12:40 UTC). Industrial activity was brought to a halt prematurely as many workers took off in disarray, thinking it was a bomb explosion. For another two minutes, what was described as a greyish-white smoke trail and a compact dust cloud was visible in the otherwise clear sky. Several eyewitnesses described the falling of stones which were accompanied by sounds like gun fire. Many observers noticed the dust cloud, but only two accounts mention the meteor.

Eight eyewitnesses were interviewed, all of whom seem to refer to the smoke trail and dust cloud. The directional data obtained by a compass and altitude-measuring device are given in Table 1.

The Meteorite Impacts

A rain of stones came down in and near Mbale, causing surprisingly minor damage to buildings and no serious injuries (Table 2). Stone No. 6 hit the roof of the local railway station and caused a 15-cm wide hole. Stone No. 9 hit the roof of a cottage. A third stone, No. 10, smashed into a cotton factory and broke into pieces when it hit metal. (This stone is currently at The Smithsonian Institution in Washington D. C.) A young boy reported that he was hit on the head by a small meteorite of 3.6 g (No. 23; Fig. 1). The stone was slowed down by the leaves of a nearby banana plant from an initial impact velocity which must have been about 30 m/s. Because of this, he fortunately remained in a position to recover the stone.

Table 1. Summary of eye witness accounts of the smoke trail.†

	X Y (km)	$(Az,H)_{begin}$ ^{o})	$(Az,H)_{end}$ ^{o})	Notes:
A.	30.5 119.4	-.- -.-	220 60	cloud 4° diameter[1]
B.	29.0 117.0	120 70	160 0[2]	-
C.	21.5 121.0	270 60	320 40	sound of gunfire
D.	27.5 119.5	200 40	300 40	cloud
E.	30.8 121.8	80 60	85 55	cloud, grey trail
F.	21.3 121.3	-.- -.-	240 60	explosion
G.	53.7 149.0	-.- -.-	70 30	cloud[3]
H.	30.4 118.6	-.- -.-	20 80	explosion

† The coordinate grid (X,Y) is in units of 1 km, with an origin at longitude 33.900°, latitude 0.000°. Azimuth is measured from the south through west.
1 Two fingers at arm length, by comparison to a silmilar sized cloudlet.
2 Direction towards which meteorites may have fallen.
3 Parallel to a distant mountain limb.

Diameters and depths of several impact pits are given in Table 2. There is a general proportionality with meteorite mass: $D = 13.1\ M^{0.51 \pm 0.10}$ cm, which is not significantly different from the expected behaviour: $D \sim M^{0.45}$ (Melosh, 1989). There is no systematic orientation in the shapes of the impact pits, which could give information on the azimuth direction of the atmospheric entry. It should be noted, however, that some of the large pits were widened while recovering the meteorite, and for some other impact pits the shape was determined by irregularities in the structure of the surface. In one case (No. 3), a stone hit the ground 1.5 m south of a 3-m high wall, indicating a nearly vertical path (H > 63°) shortly before impact.

All meteorites are fully covered by fusion crust, unless there is good evidence that the fragment was broken at, or usually after, impact. Even the smallest meteorite, which weighs only 0.10 g, was fully covered by a fusion crust before a small part was removed to check the inside structure. The interior is grey: the irregularly shaped stone consists of silicate matrix material and is not merely a troilite or Fe-Ni inclusion. The fusion crusts show no clear signs of a flow pattern, with the exception of fragment 17a. Fragments with <50% melting crust exist for at least the stones No. 2, 3, 4, 5, 12, and 49, which were reported to be broken into pieces soon after the find.

The Strewn Field

The locations of most of the 46 impacts, and two doubtful ones (No. 14 and 27), were determined by taking the finder back to the impact location (Fig. 2). The stones fell during a wet season, and at the time a large part of the relevant area was inaccessible due to high grass vegetation and damp soil. The meteorites were found in small villages, along the many narrow pathways that cross these marshes, and close to the railway tracks. There are enough of such areas to argue that the general orientation of the strewn field is well determined.

The general pattern is in a NW to SE orientation, with the largest fragments in the SE. However, the largest fragments (masses above 2 kg) are found in a more North to South oriented pattern: the fragments 15, 48, and 49 are due South of 13, 14, 21, and 12 (Fig. 2). Another feature of the pattern is that very small fragments (0.1–10 g) were found significantly westward of the main pattern. Fragments 22–25 (0.1–4 g) were found 4 km westward of fragments 37 and 39 (21 and 31 g). Fragments 17a–d were found "about 2 miles West from the BCU coffee factory" (which is located near fragment 29). There is no information about the relative location of these samples. It is possible that the more heavy fragment, 17a (135 g), was found elsewhere, but the latter stands out in being the only fragment with a clear flow pattern (see below Fig. 6).

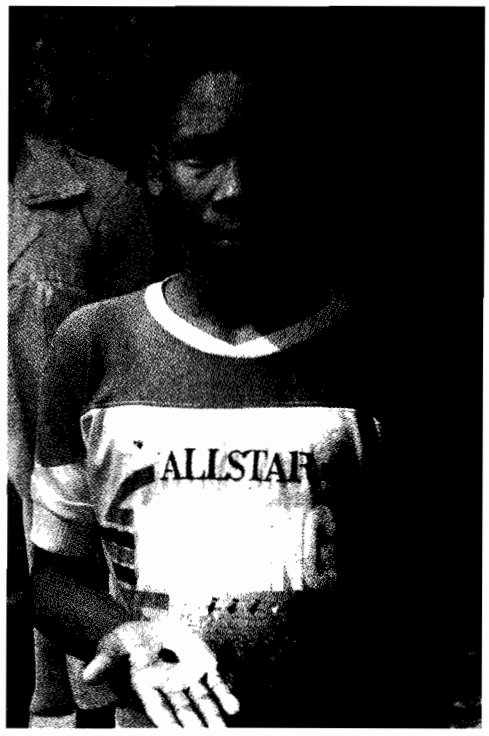

FIG 1. This young boy is the first to survive the common fear of a meteorite fall, that is, to be hit on the head. The meteorite, No. 23 weighing 3.6 g, was slowed down by the leaves of a banana plant.

Description and Classification

The Mbale is an ordinary chondrite. Analysis at Makarere University determined the density at aproximately 3.5 g/cm³. In thin sections, the predominant mineral is olivine. Some of its larger grains are subhedral, but all are cracked and fragmental. Chondrules count for 20% (in some areas up to 40% of the total volume. Their size varies between 0.4 and 1.00 mm. About 15–20% of the rock are opaques inferred to be Fe-Ni alloy and troilite. The opaque phase sometimes has olivine inclusions and shows Fe staining in surrounding grains.

A. El Goresy (Max-Planck-Institut für Kernphysik in Heidelberg) determined the mean olivine composition to be Fa = 25.4 and pyroxene Fs = 21.8 and classified the meteorite as an ordinary chondrite L6/5. This result was confirmed by P. W. C. van Calsteren (Open University in Milton Keynes, U. K.), who found Fa = 24.7 ± 0.4 and Fs = 21.3 ± 0.3. The olivine and orthopyroxene compositions are homogeneous. Results of his microprobe analysis are summarized in Table 3. R. P. Kuijper and C. E. S. Arps (National Museum of Natural History in Leiden, The Netherlands) communicated that the majority of chondrules are ill-defined, deformed and/or (partly) recrystallized. Many tend to

merge with the granular matrix. With respect to texture, most chondrules are spherulitic, barred, or granular, rather than consisting of (monomineralic) aggregates of idiomorphic crystals. The mesostasis within the barred and granular chondrules is generally very fine grained with a dusty appearance and incidentally clear. Well-defined, undeformed chondrules are scarce. Locally a chondritic structure is barely discernible, often the result of deformation effects. Effects of shock metamorphism are clearly visible (*e.g.*, strong undulatory extinction, crack systems, finely brecciated fractures, *etc.*). But no clear traces of melt phase have been observed.

Characteristic black veins are found throughout the stones. Their general orientation is most clearly seen in the large fragment No. 13, where the crust is missing (Fig. 3). The veins are seen in a more or less parallel orientation. Microprobe analysis at the Kamerlingh Onnes Laboratory in Leiden (Ton Gortemulder) did not reveal a large compositional variation across the veins, indicating shock induced deformation. A large number of the fragments show an angular habit with rounded edges and nearly flat surfaces (Fig. 4), which is different from some irregular surfaces seen on No. 13. This suggests that preferential break-up occurred along the black veins during entry into the Earth's atmosphere and the irregular part of No. 13 is the remnant of the crust before the major breakup event. However, only one surface of one fragment shows remains of the dark vein material.

TABLE 2. A summary of impact positions, masses of fragments, diameter (D) and depth of any impact pits and notes on field condition and circumstances of the find.†

No.	X (km)	Y (km)	mass (kg)	D (cm)	depth (cm)	remarks:
1	29.130	119.180	5.6	10	-.-	P, on pavement road
2	28.425	118.450	(0.5)	-.-	-.-	D, prison area
3	28.510	118.480	(8)	50	60	D, damp clay
4	28.490	118.665	(1.5)	25	-.-	D, dry field
5	28.570	118.710	(1)	*)	-.-	D, damp clay
6	28.575	119.117	(1)	-.-	-.-	B
7	28.160	119.170	(1.5)	15	-.-	P,in sand on fuel depot
8	28.280	119.490	(1)	-.-	-.-	M, between houses
9	28.210	119.500	(2)	-.-	-.-	M, on roof house
10	28.760	119.430	10-15	25	-.-	B, concrete floor
11	29.950	118.680	(1)	15	-.-	M, dry field garden
12	28.910	117.750	(10)	*)	-.-	D, damp clay
13	28.340	117.910	27.4	150	-.-	swamp, damp clay
14	28.420	117.960	?	*)	-.-	M, doubtful
15	28.170	117.230	11.8	50	85	in forest, damp clay
16	28.560	119.120	0.685	-.-	-.-	
17a	23.7	119.1	0.1349	-.-	-.-	on the road
17b	-	-	0.0283	-.-	-.-	as 17a
17c	-	-	0.0035	-.-	-.-	as 17a
17d	-	-	0.0021	-.-	-.-	as 17a
18	27.490	119.400	2.0	-.-	-.-	
19	27.180	120.650	(0.5)	-.-	-.-	M, rice field
20	27.000	120.600	0.3957	-.-	-.-	cassave field
21	28.670	117.750	(2)	*)	-.-	M
22	22.875	121.250	0.0047	-.-	-.-	in village
22a	-	-	0.0007	-.-	-.-	in village
22b	-	-	0.0001	-.-	-.-	in village
23	22.525	121.300	0.0036	-.-	-.-	fell on boy's head
24	22.675	121.250	0.0011	-.-	-.-	open field
25	22.875	121.400	0.0007	-.-	-.-	between houses
25a	-	-	0.0003	-.-	-.-	as 25
26	27.135	119.270	0.500	-.-	15	hit banana plant
27	27.250	119.280	(0.5)	-.-	-.-	M, doubtful
28	27.310	119.350	3.2	-.-	-.-	impact hole in field
29	27.310	119.320	0.2317	-.-	-.-	on the road
30	27.215	119.335	(0.4)	-.-	-.-	
31	27.630	119.005	1.2487	-.-	-.-	in rice field
32	27.425	119.170	0.0971	-.-	-.-	in rice field
33	27.225	119.300	0.3803	-.-	-.-	on the road
34	27.445	119.600	0.2050	-.-	-.-	in grass
35	27.330	119.590	0.3172	-.-	-.-	in grass
36	27.540	120.085	(0.2)	-.-	-.-	M, in village
37	26.775	121.575	0.0204	-.-	-.-	under banana plant
38	27.350	121.000	(0.5)	-.-	-.-	M, rice field
39	27.100	121.525	0.0307	-.-	-.-	
40	28.500	119.240	0.1353	-.-	-.-	
41	27.630	119.415	0.0559	-.-	-.-	
42	27.380	119.390	0.0560	-.-	-.-	
43	27.330	119.410	0.7050	-.-	-.-	fell on railway
44	27.180	119.290	0.6920	-.-	-.-	on the road
45	26.970	119.250	0.1453	-.-	-.-	on the road
48	28.210	116.800	5.6	*)	-.-	swamp
49	28.838	116.940	(3)	40	10	D, swamp
50	27.3?	119.3?	0.3326	-.-	-.-	gamma spectroscopy

† Masses between brackets: estimate only, the mas could not be measures.
*) impact pit reported, no information available.
B broke up during impact.
D reported as being destroyed.
P in private collection.

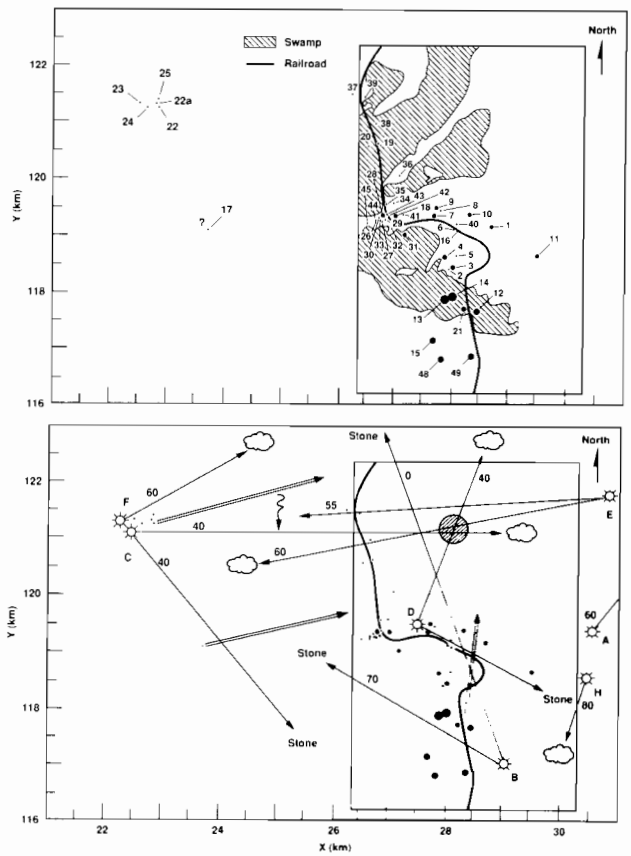

FIG 2. The location of 48 masses is shown superposed on a map of the surroundings of Mbale. The upper plot gives numbers, in order of find, that refer to Table 2 and shows the wet area that was mostly inaccessible for research during the expedition. The lower plot summarizes directional information regarding the smoke trail and dust cloud seen by eye witnesses shortly after the explosion was heard. Final fragmentation occurred above X = 28.2, Y = 121.1. Double arrows trace the path of some stones by wind drift and residual cosmic velocity back to the explosion point (general direction only).

FIG. 3. Largest fragment No. 13. Scale bar in units of 1 cm. The part containing melting crust is irregular with thumb print depressions. Where the crust is missing, thin shock veins can be seen in a parallel orientation.

Recent Ar-Ar analysis of a Mbale whole rock sample by one of us (JK) preliminary yields a plateau age of about 500 Ma indicating that this fall may belong to the family of L-chondrites with rather young age, among which is the L6 chondrite Bruderheim (see *e.g.*, Turner, 1988). This age is thought to be not the crystallisation age of the meteorite but the point in time when the K-Ar system of this rock was severely disturbed by reheating, most probably due to a great collision event that its parent body suffered in the asteroid belt. We speculate that this event may be associated with the formation of the shock veins.

TABLE 3. Results of microprobe analysis.†

	Olivine (Wt %)	σ	Orthopyroxene (Wt %)	σ
SiO_2	38.6	(0.5)	55.7	(0.5)
TiO_2	0.03	(0.01)	0.19	(0.03)
Al_2O_3	-.-		0.12	(0.03)
FeO	22.31	(0.12)	13.63	(0.13)
MnO	0.49	(0.01)	0.49	(0.02)
MgO	38.2	(0.8)	28.3	(0.2)
Cr_2O_3	0.01	(0.02)	0.10	(0.04)
NiO	0.01	(0.03)	-.-	
Total	*99.7*	*(0.8)*	*98.4*	*(0.6)*

† Data are given for a mean of 7 olivine and 11 orthopyroxene analyses. Wt% oxide. Standard deviations are in parentheses (courtesy of P. W. C. van Calsteren).

MASS ESTIMATES

The Total Recovered Mass

The total recovered mass, as of 1993 October, is derived from the following bookkeeping of the reported finds. Prior to and during the expedition, 2.02 and 52.88 kg of material was recovered.

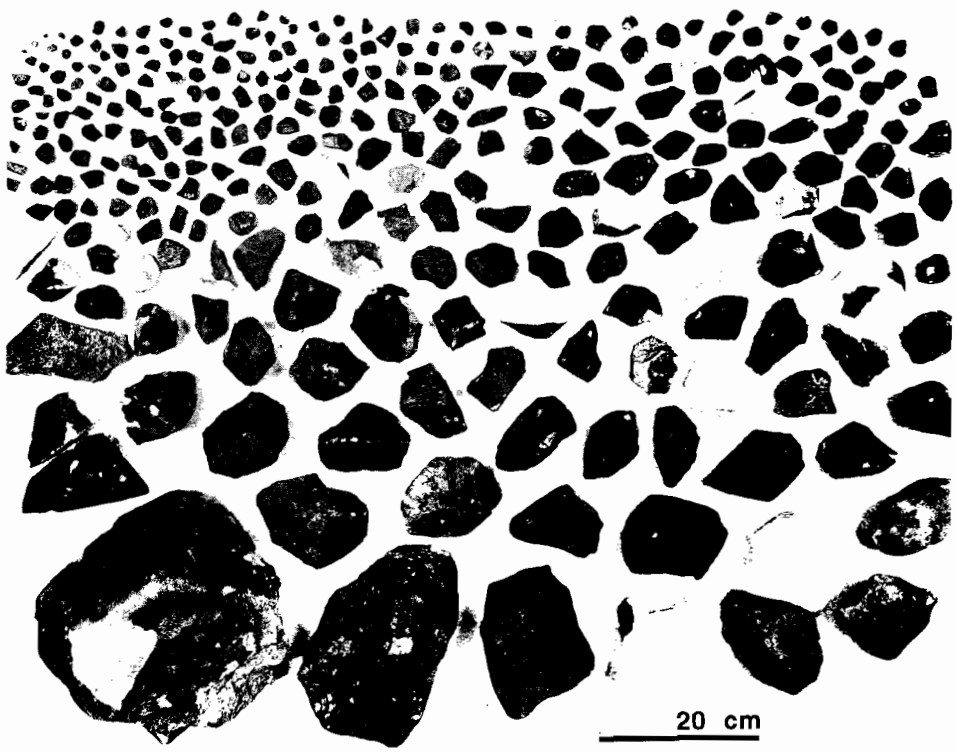

FIG. 4. Collection of a large number of fragments of Mbale. The largest mass (27.4 kg) is shown at the bottom left, the smallest mass (0.1 g) at the top left. Note the angular appearance of many large fragments.

In the months after the rainy season, another 41.48 kg of material was gathered by the local population, mostly in the form of small fragments. A rumour prevails that a large mass of 30–50 kg exists, possibly from impact position No. 14. Recent attempts to recover a mass in this apparent impact pit were fruitless. American prospectors obtained about 14.2 kg through a trader who visited the city shortly after the fall. Independently, 12.77 kg of material was acquired by the Swiss Meteorite Lab in 1992 December. More recently, some 437 specimens (26.18 kg) were bought from the local people by a Mbale dealer. This adds to a certain recovered mass of 149.5 kg. Missing fragments, notably fragment No. 14, adds another 50 kg of possible material.

The Total Fallen Mass

The total fallen mass can be estimated from the mass distribution of individual fragments. Although no information is available on the impact location, mass estimates were obtained of 426 fragments with more than 50% fusion crust in our collection and the 437 speciments mentioned above. The resulting distribution (Fig. 5) is smooth and close to what is expected for a single catastrophic fragmentation (solid line). The down turn at low masses is real. Less certain is if the peak near 0.02 kg is significant. If so, it implies small scale fragmentation prior to the main breakup event. However, a false peak can occur if a particular area in the strewn field has higher recovery probability than elsewhere.

Catastrophic fragmentation results in a mass distribution such that

$$\Delta N(M) * M \sim M^{+k/3} \Delta (\log M),$$

with k = 1.2 for diameters larger than 0.1x the diameter of the original mass (M_∞) and a factor of 2 smaller for smaller fragments (Fujiwara *et al.*, 1989). The actual distribution falls only a little short of this trend, down to masses of 0.01 kg. The total fallen mass (M_f) may be estimated from the area beneath the curve, which amounts to 195 kg. Most of this mass is in the large fragments. We are confident that in spite of the harsh terrain, most, if not all, large fragments have been recovered, because the largest fragments (5–50 kg) left clear impact pits even in muddy areas. It is unlikely that these large stones sunk out of sight. The possible existence of a large mass on position 14 adds significantly to the uncertainty in our final estimate of the total fallen mass: $M_f = 190 \pm 40$ kg.

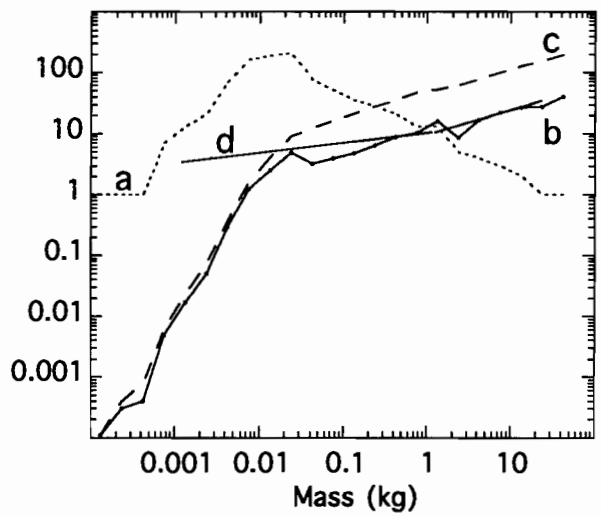

FIG. 5. Mass distribution of recovered fragments with > 50% fusion crust. The diagrams shows (a) the number of fragments per bin of 1/4 decade in mass. (b) The total mass per bin. (c) The cumulative mass distribution. (d) Line d is an expected distribution for a single catastrophic collision.

The Initial Mass Derived From Gamma Ray Spectroscopy

As a result of the efforts of J. Betlem (IUCN, World Conservation Union, Mbale), a specimen of 332.6 g was available for γ-ray spectroscopy at Heidelberg within 12 days of the fall so that cosmogenic radionuclides with short lives could be detected (*e.g.*, ^{52}Mn). Unfortunately, the exact location of this specimen in the strewn field is unknown, but judging from its mass and the strong mass segregation seen in the strewn field, it must have fallen near fragments 29 and 33. A second specimen was measured later, 46.3 g of a fragment that is from a heavy (M ~ 8 kg) specimen, probably No. 3. These samples were sent to Europe for analysis in the days before the field expedition (Table 4).

The level of activity for the shortest living isotope ^{52}Mn, with $t_{1/2}$ = 5.6 days, was found to be 17 ± 5 dpm/kg, which is in good agreement with data for the Torino H6 fall (20.3 ± 1.8), the Lost City H5 (34 ± 11), the Aomori L6 (14 ± 4), the Saint-Severin (15 ± 6) and the recent L6 fall Mohonoseki (21 ± 2.5) (Bhandari *et al.*, 1989; Cressy, 1971; Yabuki *et al.*, 1985; Bibron *et al.*, 1974; and Shima *et al.*, 1993 respectively). To our knowledge, no further data are presently available.

The production rate of cosmogenic nuclides in a meteorite depends on the size of the meteoroid, its chemical composition, and the shielding depth within it. All relevant nuclides except ^{60}Co (and ^{40}K, U, and Th, which are primordial) are mainly produced by spallation reactions which cause a steep rise of the rate at shallow

TABLE 4. Low level radionuclide activity, in dpm/kg, at the time of fall.†

isotope	$t_{1/2}$	No. 3 46.3 g	No. 50 332.6 g	Mohonoseki 6.38 kg
^{52}Mn	5.59d	-.-	17±5	21±2.5
^{48}V	15.98d	33±20	18±6	15±2
^{51}Cr	27.70d	<80	37±14	57±12
^{7}Be	53.29d	71±25	60±11	62±7
^{58}Co	70.78d	11.8±4.1	4.5±1.5	3.3±0.7
^{56}Co	77.28d	<8	6.0±4	8.9±0.5
^{46}Sc	83.83d	5.4±3.5	6.0±2	5.8±0.5
^{57}Co	271.8d	15.4±2.0	7.4±1.3	6.5±1.1
^{54}Mn	312.5d	105.3±6.5	56.7±3.5	47±1
^{22}Na	2.602y	100±7	64.5±3.9	61±1
^{60}Co	5.27y	34.0±2.0	<1.5	0.3±0.3
^{26}Al	7.16×10^{5}y	76.4±5.0	54.8±3.3	46±1
Th	1.405×10^{10}y	15.6±6.1	8.9±1.8	-.-
U	4.47×10^{9}y	14.8±3.7	6.7±1.4	-.-
^{40}K	1.28×10^{9}y	1782±107	1686±105	1598±16

† The specimen labeled No. 3 is a fragment of one of the main masses. Its identification is not certain.

The Th, U, and K concentrations of No. 50 correspond to 36 ppb, 9ppb, and 909 ppm respectively.

Specimen No. 50 was probably found close to fragments 30, 32, and 33. The data for this surface fragment are in good agreement with those of the small L6 chondrite Mihonoseki, which fell on 1992 December 10 (data from Shima *et al.*, 1993).

shielding depth due to a fast buildup of the secondary nuclear cascade. Maximal production occurs at the center of a stone meteoroid of radius R = 40–70 cm. However, ^{60}Co is produced by slow neutron capture on ^{59}Co. Since the slowing down of secondary neutrons is strongly mass dependent, ^{60}Co is highly sensitive to size and depth. Only at radii above about 20 cm does its production become effective and reach its maximum for R ~ 80 cm with a rather slow increase from the surface to the center (Eberhardt *et al.*, 1963). The fact that the ^{60}Co activity of both samples differs largely indicates that the pre-atmospheric Mbale was rather large. According to the model calculations of Eberhardt *et al.*, the production of 34 dpm/kg of sample No. 3 can only be reached for radii larger than R = 30 cm.

Sample No. 50 was close to the surface. The lower shielding of this sample is also confirmed by the lower spallation activities. From the presumed location of No. 50 in the strewn field, it is hoped that samples even closer to the original surface can be identified. This would allow us to study cosmogenic production at the transition from solar flare to galactic cosmic ray ranges (*e.g.*, Evans *et al.*, 1982).

It is possible to estimate an upper limit to the mass of the meteoroid before entry in the atmosphere by assuming that all masses with M > 1 kg came from a spherical core, and fragment No. 3 was on the outer surface of this core. The core would have a radius of 23 cm (or 25 cm if the 50 kg mass exists). A total radius of about 40 cm gives the correct shielding depth to produce 34 dpm/kg ^{60}Co at 23 cm from the center of the core. The possible extra core mass of 50 kg hardly changes this result: it would imply a mass of some 1050 kg, instead of 960 kg. It must, however, be pointed out that for simplification the model calculations are based on spherical geometry. We tentatively conclude from the cosmogenic radionuclide data that the pre-entry mass (M_∞) was larger than 400 kg (R = 30 cm) and not much more than 1000 kg (R = 40 cm). The lower mass limit assumes that the 46.3-g sample was in the center of the pre-entry meteoroid.

DIRECTION OF FLIGHT OF THE METEOR

The position of individual specimens in the strewn field gives information about the atmospheric trajectory of the meteor, after correction for wind drift.

Correction for Wind Drift

Atmospheric wind velocity data were obtained from the European Centre for Medium-Range Weather Forecasts (ECMR) at Reading, England. Data for altitudes between 0.12 and 31.1 km are available for a 2.25° grid in longitude and latitude at 12 h UTC and 18 h UTC. We have taken the values at 12 h UTC and linearly interpolated the data for gravitation potential, temperature, and X, Y, and Z velocities to the approximate position of the meteorite (Table 5). Negligible errors occur if the trajectory of the meteor was different from that assumed. The wind vector points in an ESE direction below 5 km altitude and in an approximate WSW direction above 5 km altitude. The wind pattern is qualitatively consistent with the observed distribution of masses it only if the breakup occurred significantly above 5 km altitude.

The horizontal displacement was calculated by solving the drag equation for each specimen with mass M and radius R, where the instantaneous force (F) on the stone is given by:

$$F = \frac{1}{2} C_\omega \pi R^2 \rho_{air} V^2 - Mg$$

TABLE 5. Atmospheric wind profile at the approximate position of the meteor.†

Z (m)	T (K)	P (Pa)	V_x (m/s)	V_y (m/s)	V_z (m/s)
121	304.74	100,000	+3.402	-0.836	+0.176
789	300.83	92,500	+3.437	-0.829	+0.168
1,514	296.59	85,000	+3.550	-0.812	+0.027
3,161	281.80	70,000	+3.983	-1.776	-0.541
5,869	267.14	50,000	-5.911	+1.198	+0.521
7,592	257.67	40,000	-7.720	+2.236	+0.356
9,684	238.98	30,000	-9.200	-4.678	+0.147
10,933	228.58	25,000	-15.904	-6.672	+0.071
12,393	219.73	20,000	-13.801	-3.760	+0.065
14,194	206.66	15,000	-2.413	-9.540	+0.017
16,556	197.33	10,000	-15.655	-0.461	-0.020
18,660	204.62	7,000	-10.560	-1.358	+0.004
20,697	208.40	5,000	-17.768	+2.586	-0.014
23,901	218.53	3,000	-2.677	-3.767	-0.009
31,084	229.69	1,000	+7.467	+4.899	+0.002

†Values of temperature (T), pressure (P), and wind velocity (V) are given as a function of altitude (Z).

Data are derived from the ECMWF/Tropical Ocean and Global Atmosphere-Advanced Upper Air Data Set for 12 UTC on 1992 August 12.

where V is the velocity, ρ_{air} the air density, and g the gravitational deceleration at the instantaneous altitude. Trajectories were calculated for an adopted drag coefficient C_ω, a breakup height, and a direction and magnitude of the velocity prior to dark flight (*e.g.*, McCrosky *et al.*, 1971; Smith and Stammers, 1973).

The drag coefficient C_ω depends on the shape of the meteorite, surface roughness, Reynolds number, and orientation during the fall. Values for relevant Reynolds numbers and for smooth spheres and cylinders of small axis ratio are in the range 0.2–0.5. Results from photographically recorded tracks of meteors, however, show C_ω in the range of 1.2–1.8 (*e.g.*, Sekanina, 1993). An average C_ω can, in principle, be derived from the impact velocity which in turn is derived from the impact pit diameters (*e.g.* Fechtig *et al.*, 1980), but good calibration is lacking.

Fortunately, it is possible to make a statement without knowing the exact instantaneous value of C_ω along the trajectory, because the largest fragments (3–30 kg) are hardly affected by the wind for any reasonable value of C_ω. Their relative location reflects the movement of the meteor, which should have been from a direction Az ~ 168–185° (*i.e.*, from the North), or from somewhat higher aximuth if C_ω is larger than 0.2. On the other hand, the smallest fragments (M < 0.2 kg) quickly lose their initial velocity and then follow a ground-projected trajectory in a WSW direction for any initial altitude above 8 km. The double arrows in Fig. 2 trace this path backward.

Because all displacements are relative to the point where breakup occurs, we first tried to determine the main breakup point. The eye witnesses were located in a suitable way to determine the position of the final breakup point. The visual observations (Table 1) refer to the dust cloud and not to the fireball. Observations C, D and E converge at a point at X = 28.2, Y = 121.1. This positions aligns with the orientation of the main masses (M > 1 kg). The altitude of the event is certainly higher than the 2.5 km inferred from these observations. From a similar study of the Glanerbrug

meteorite fall, we found that the observers close to the impact point tended to underestimate the height of a phenomenon in the sky (Jenniskens *et al.*, 1992b). Observers A, H, and F put the event higher up in the sky (60−80°), which is probably correct, but they seemed to lose a sense of direction. The high position on the sky may have confused the observers because few good reference points are available. The height estimates of observers A, H, and F result in altitutes of 5.4 km, 19.3 km, and 10.0 km, respectively, if the event happened above X = 28.2, Y = 121.1. Observer G, who was farther away, indicated an altitude of 15 km (with considerable uncertainity). The presence of a fusion crust on all fragments indicates a breakup before the hightest deceleration occurred, that is, above 10 km altitude.

The large masses may well originate from this final breakup event. The displacement of the large masses indicates a steep trajectory (H = 60–70°) and a remnant velocity during breakup of less than 0.1 km/s. Reasonable solutions for smooth spheres exist where the large mass of 27.4 kg is less far displaced than masses of 5 kg, as is observed.

This location of the final breakup point cannot account for masses less than 1 km. Starting from the breakup point, all fragments move to some extent parallel to the ground-projected trajectory of the meteor, where the displacement depends on the remnant (cosmic) velocity, and simultaneously all fragments are blown away from that trajectory by the wind. Therefore, masses No. 37 and 39 should originate from a point more to the North. A reasonable solution exists, with C_ω as for a sphere (and a function of the Reynolds number), for a breakup at 20 km, and a remnant cosmic velocity of 4 km/s. From photographed meteorite falls, it has been found that the velocity of some heavier fragments (~10 kg) is still of order 2–6 km/s at 20 km altitute (*e.g.*, Wetherill and ReVelle, 1981). In that case, the sideward displacement is about 1.7 km.

FIG. 6. Flow pattern and irregularities in the fusion crust of fragment No. 17 a.

The relative location of fragments 22–25 (1 g) cannot be understood even for a breakup much higher than 20 km. Only if the drag coefficient C_ω is larger than 1.2 is there enough displacement in a westward direction to account for the large separation with respect to masses 37 and 39. A breakup at about 30 km altitude with remnant velocity of order 12 km/s can account for the large westward displacement of these small masses and the relative position with respect to fragments No. 37 and No. 39. Again, the calculations indicate a steep entry angle, of order H = 65°, or somewhat less if the smallest fragments stayed in the wake of the main mass for some time. Also, masses No. 17 a–d must have an origin high in the atmosphere, early in the descent, which is consistent with the observation that fragment 17a is the only relatively large fragment (135 g) with a clear flow pattern in the fustion crust (Fig. 6). The presence of a well-developed flow texture on this fragment indicates that it predates most of the other crusted surfaces and that this fragment way have especially interesting cosmogenic properties.

This pattern of events indicates that the entry angle is relatively large, of order 65°. Visual observer G indicated a relatively shallow entry ("parellel to a distant mountain limb"). This observation may not be very reliable (again see Jenniskens *et al.*, 1992a, for a comparison of such estimates from visual observations of a similar event), and it is not clear if this argues against a path as steep as 65° The trajectory in the Earth's atmosphere is probably not determined better than: AZ = 170–200°, H = 40–70°.

PRE-ENTRY ORBIT

In order to calculate the orbital elements, an estimate of the size of the entry velocity is needed. The entry velocity may be estimated from the amount of ablation comparing the initial pre-entry mass (M_∞) and the final fallen mass (M_f). The amount of mass lost due to ablation is:

$$M_f = M_\infty \exp(-\sigma V_\infty^2 / 2)$$

(Wetherill and ReVelle, 1981), where σ = 2.0 x 10^{-8} sec^2/m^2 as derived for the Lost City and Innisfree meteorites. From the estimates of M_f = 150−230 kg and M_∞ = 400−1000 kg, and the minimum entry velocity of 11.2 km/s caused by the gravitational pull of the Earth, we have V_∞ = 11.2−13.8 km/s (most likely 12.9 km/s).

This completes the data necessary to calculate the orbital elements. As said previously, the trajectory in the Earth's atmosphere is probably determined not better than: Az = 185 ± 15, H = 55 ± 15, and V_∞ = 11.2−15 km/s, with most likely values Az = 185, H = 65m and V_∞ = 13 km/s. But this does limit the possible orbital elements of the meteoroid to a small range in perihelion distance (q = 0.94−0.99 AU), inclination (i = 4−14°) and argument of perihelion (ω) as shown in Table 6. These values are similar to the mean parameters derived from MORP and PN fireballs that may have dropped meteorites: q = 0.98 AU and i = 6.9° (Wetherill and ReVelle, 1981; Halliday *et al.*, 1989).

The eccentricity of the ellipse is less well determined (e = 0.06 −0.51). Previous observations indicate that the eccentricity of meteorite producing orbits peak in a relatively narrow range around e ~ 0.50 (0.42−0.67) (Jenniskens 1992a), although Bruderheim, in

some respects a fall similar to Mbale, had e ~ 0.25 (Follinsbee, 1961). Earth crossing asteroids have eccentricities usually larger than e = 0.2 (*e.g.*, Wetherhill, 1985; Greenberg and Nolan, 1989). If this is true for Mbale, it implies that the entry velocity was 13–15 km/s. From Eq. (2), it follows then that $M_f/M_\infty \sim 0.10-0.18$ or M_∞ is close to 1000 kg. Because the perihelion distance is well determined, this constrains the semi-major axis to a ~ 1.2–1.9 and the aphelion distance Q ~ 1.4–2.8 AU.

The orbit reaches out to the inner part of the asteroid belt (Fig. 7), which allows a scenario with a short time interval since the meteoroid was captured in a non-resonant orbit by the Earth. However, the more likely small value of e (e ~ 0.2–0.4), in combination with a perihelion distance close to q = 1.0, suggests that the meteoroid evolved due to multiple encounters with the Earth, along surfaces of constant Tisserand invariant, for a period of order 10^7 yr (Greenberg and Nolan, 1989).

CONCLUSION

The study of the Mbale meteorite fall has resulted in a fair estimate of the orbit before entry in the Earth's atmosphere, which adds to a small number (about 15) of reasonably well determined orbits of meteorite-dropping events. We have as most likely values: a = 1.37 ± 0.20, q = 0.96 ± 0.2, e = 0.30 ± 0.10, i = 8 (6–14)°, Ω = 142°, and ω = 139 ± 11°, which describe the orientation and shape of the orbital ellipse in space (Fig. 7). The orbit was derived not from eye witness accounts, which were difficult to obtain, but from the study of the strewn field in combination with γ-ray spectroscopy of several fragments. The location of different masses in the strewn field defines the trajectory of the meteor in the atmosphere, while the ^{60}Co data give useful constraints on the initial mass before entry. In combination with a good estimate of the total fallen mass and an ablation coefficient as found from other chondrite falls, this constrains the entry velocity. Trajectory and entry velocity define the orbit in space.

The breakup process during descent in the atmosphere is complex. The smaller fragments, 22–25, broke up at higher altitude than the larger, 37 and 39, and a final breakup may have produced the largest fragments with masses larger than 1 kg. Preferential breakup possible occurred along the shock veins found throughout the meteorite. The breakup process is the subject of a more elaborate study conducted at the MPI für Kernphysik in Heidelberg, in which ^{60}Co is used as a tracer of depth in the meteoroid before ablation and breakup.

TABLE 6. Orbital elements of the Mbale asteroid for a range of representative values for the trajectory and entry velocity.

V_∞ (km/s)	Az °)	H °)	a (AU)	q (AU)	e	i °)	ω °)	Q (AU)
12	170	45	1.00	0.92	0.08	7	74	1.08
12	190	45	1.02	0.96	0.06	7	95	1.08
12	190	55	1.09	0.98	0.10	6	128	1.20
12	170	65	1.11	0.96	0.14	4	123	1.27
12	180	65	1.13	0.97	0.14	5	132	1.29
12	190	65	1.15	0.98	0.15	5	141	1.32
12	200	65	1.18	0.99	0.16	5	149	1.37
15	170	45	1.20	0.90	0.26	14	116	1.51
15	190	45	1.29	0.94	0.27	14	131	1.64
15	190	55	1.49	0.95	0.37	12	139	2.04
15	170	65	1.54	0.92	0.41	8	132	2.17
15	180	65	1.63	0.94	0.42	9	138	2.31
15	190	65	1.73	0.95	0.45	9	144	2.51
15	200	65	1.85	0.97	0.48	9	150	2.74
15	190	75	1.95	0.95	0.51	6	146	2.94

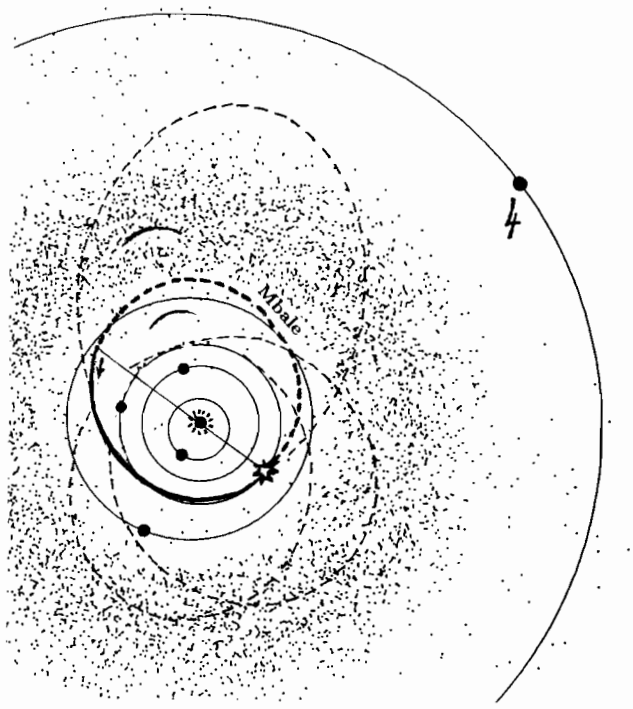

FIG. 7. The orbit in space. Two arcs show the uncertainty in aphelion distance. Dashed lines are photographically recorded orbits of Pribram, Lost City, and Innisfree (after Halliday *et al.*, 1978) and all are projected on the distribution of known asteroids on 1988 March 8 (from McFadden *et al.*, 1989).

Acknowledgements–The expedition that studied the Mbale strewn field is a collaboration of the Leiden University and Makarere University which was made possible by Dr. Harm Habing, Director of the Leiden Observatory. Many local officials in Uganda were helpful and assisted where necessary. Support was given by the Mount Elgon Conservation and Development Project in Mbale. Dr. René Kuiper (DeSitter Fonds, Leiden) enabled communications with Uganda. Funding was obtained from Het Leids Kerkhoven-Boscha Fonds (Dr. Jan Lub), the National Museum of Natural History in Leiden (Dr. C. E. S. Arps), and the Max Planck Institute für Kernphysik at Heidelberg (Dr. Elmar Jessberger, Dr. Till Kirsten and Dr. Wolfgang Hampel). The paper benefited from contributions by Dr. A. El Goresy (MPI für Kernphysik in Heidelberg), Dr. P. W. C. van Calsteren (Open University in Milton Keynes, U. K.), and Dr. C. E. S. Arps (National Museum of Natural History in Leiden) and from discussions with C. R. ter Kuile (Dutch Meteor Society) and Dr. S. Davis (NASA/Ames Research Center in Moffett Field, California). The Ar-Ar measurements were made possible by Dr. Elmar Jessberger (MPI für Kernphysik). The atmospheric wind data were obtained with the help of Kathy Rider (ECMRWF, U. K.), Jan Barkmeyer (KNMI, The Netherlands), and Jacob Kuiper (Dutch Meteor Society). Also, we would like to thank Ton Gortemulder (Kamerlingh Onnes Laboratory in Leiden), Dr. Annemarie Zoete (Dutch Meteor Society) and Dr. David F. Blake (NASA/Ames Research Center) for their support of the project.

Editorial handling: R. Jones

REFERENCES

BARIFAIJO E., HAMPTON C., SCHLÜTER T. AND BETLEM H. (1993) *Documenta Naturae* 77.

BEGEMANN F., ZHAOHUI LI., SCHMITT-STRECKER S., WEBER H.W. AND XU ZITU. (1985) Noble gases and the history of the Jilin meteorite. *Earth Planet. Sci. Lett.* **72,** 247–262

BETLEM H. (1992) Grote meteorietval in Mbale, Uganda. *Radiant* **14,** 75–98.

BETLEM H. (1993) The day that rained stones. *Sky and Telescope* **June,** 96–97.

BHANDARI N., BONINO G., CALLEGARI E., CINI CASTAGNOLI G., MATHEW K.J., PADIA J.T. AND QUEIRAZZA G. (1989) The Torino, H6, meteorite shower. *Meteoritics* **24,** 29–34.

BIBRON R., LEGER C., TOBAILEM J., YOKOYAMA Y., MABUCHI H. AND BAILLARD N. (1974) Radionuclides produits par le rayonnement cosmique dans la météorite Saint-Séverin. *Geochim. Cosmochim. Acta* **38,** 197–205.

CEPLECHA Z. (1961) Multiple fall of Pribram meteorites photographed. *Bull. Astron. Inst. of Chech.* **12,** 21–47.

CRESSY P. J. (1971) Cosmogenic radionuclides in the Lost City and Ucera meteorites. *J. Geophys. Res.***76,** 4072–4075.

EBERHARDT P., GEISS J. AND LUTZ H. (1963) Neutrons in meteorites. In *Earth Science and Meteoritics* (eds. J. Geiss and E. P. Goldberg), pp.143–168. North-Holland Publishing Co., Amsterdam.

EVANS J. C., REEVES J. H., RANCITELLI L. A. AND BOGARD D. D. (1982) Cosmogenic nuclides in recently fallen meteorites: Evidence for galactic cosmic ray variations during the period 1967-1978. *J. Geophys. Res.* **87,** 5577–5591.

FECHTIG H. NAGEL K., PAILER N. AND SCHNEIDER E. (1980) Collisional processes of iron and steel projectiles on targets of different densities. In *Solid Particles in the Solar System* (eds. I. Halliday and B. A. McIntosh), pp. 357–363. D. Reidel, Boston.

FOLLINSBEE R. E. AND BAYROCK L. A. (1961) The Bruderheim meteorite–fall and recovery. *J. Roy. Astron. Soc. Canada* **55,** 218–228

FUJIWARA A., CERRONI P., DAVIS D., RYAN E., DI MARTINO M., HOLSAPPLE K. AND HOUSEN K. (1989) Experiments and scaling laws for catastrophic collisions. In *Asteroids II* (eds. R. P. Binzel, T. Gehrels and M. S. Matthews M.S.), pp. 240–265. Univ. Arizona Press, Tucson, Arizona.

GREENBERG R. AND NOLAN M. C. (1989) Delivery of asteroids and meteorites to the inner solar system. In *Asteroids II* (eds. R. P. Binzel, T. Gehrels and M. S. Matthews), pp. 778–804. Univ. Arizona Press, Tucson, Arizona.

HALLIDAY I., BLACKWELL A. T. AND GRIFFIN A. A. (1978) The Innisfree meteorite and the Canadian camera network. *J. Roy. Astron. Soc. Canada* **72,** 15–39.

HALLIDAY I., BLACKWELL A. T. AND GRIFFIN A. A. (1989) The typical meteorite event, based on photographic records of 44 fireballs. *Meteoritics* **24,** 65–72.

HEIDE F. (1988) *Kleine Meteoritenkunde.* Springer Verlag, Berlin. 188 pp.

HEUSSER G., OUYANG Z., KIRSTEN T., HERPERS U. AND ENGLERT P. (1985) Conditions of the cosmic ray exposure of the Jilin chondrite. *Earth Planet. Sci. Lett.* **72,** 263–272.

JENNISKENS P., BOROVICKA J., BETLEM H., TER KUILE C., BETTONVIL F. AND HEINLEIN D. (1992a) Orbits of meteorite producing fireballs. *Astron. and Astrophys.* **255,** 373–376.

JENNISKENS P., BOROVICKA J., BETLEM H., TER KUILE C., BETTONVIL F. AND HEINLEIN D. (1992b) The Glanerbrug Meteorite Fall. *Astrononical Inst. of the Czechoslovak Acad. Sci. Publ.* **No. 79,** 1–17.

KRINOV E. L. (1960) *Principles of Meteoritics.* Pergamon Press, New York

MCCROSKY R. E., POSEN A., SCHWARTZ G. AND SHAO C.-Y. (1971) Lost City meteorite–its recovery and a comparison with other fireballs. *J. Geophys. Res.* **76,** 4090–4108.

MCFADDEN L., BYTOF J. AND THOLEN D. (1989) backcover of *Asteroids II* (eds. R. P. Binzel, T. Gehrels and M. S. Matthews). Univ. of Arizona Press, Tucson, Arizona.

MELOSH H. J. (1989) *Impact Cratering–A Geological Process.* Oxford Library Press, Cambridge. 245 pp.

MÜLLER N. AND JESSBERGER E. K. (1985) Dating Jilin and constraints on its temperature history. *Earth Planet. Sci. Lett.* **72,** 276–285.

NININGER H. H. (1963) Meteorite distribution on Earth. In: *The Moon, Meteorites and Comets* (eds. B. M. Middlehurst and G. P. Kuiper), pp. 162–182. Univ. Chicago Press, Chicago, Illinois.

ROBERTS R. O. (1947) Meteorites in Uganda. *Uganda Journal* **11,** 42–46.

SEKANINA Z. (1993) Disintegration phenomena expected during collision of Comet Shoemaker-Levy 9 with Jupiter. *Science* **262,** 382–387.

SHIMA M., HONDA M., YABUKI S. AND TAKAHASHI K. (1993) Cosmogenic radionuclides in recently fallen chondrites Mihonoseki and Tahara (abstract). *Meteoritics* **28,** 436

SMITH J. M. M. AND STAMMERS E. (1973) *Fysische transport verschijnselen I.* DUM, Technical Univ., Delft.

TURNER G. (1988) Dating of secondary events. In: *Meteorites and the Early Solar System* (eds. J. F. Kerridge and M. S. Matthews), pp. 276–288. Univ. Arizona Press, Tucson, Arizona.

YABUKI S., SHIMA M. AND MURAYAMA S. (1985) Cosmic-ray-produced-radioactive nuclides in freshly fallen chondrites, Aomori and Tomiya (abstract). *Meteoritics* **20,** 789–790.

WETHERILL G. W. (1985) Asteroidal source of ordinary chondrites. *Meteoritics* **20,** 1–22.

WETHERILL G. W. AND REVELLE D. O. (1981) Which fireballs are meteorites? *Icarus* **48,** 308–328.